Influences of template layer thickness on strain fields and transition energies in self-assembled SiGe/Si quantum dots

M. K. Kuo,[a] T. R. Lin, and K. B. Hong
Institute of Applied Mechanics, National Taiwan University, No. 1 Sec. 4 Roosevelt Road, Taipei, 10672 Taiwan

(Received 25 May 2007; accepted 7 January 2008; published online 2 April 2008)

This paper investigates the influence of thickness of template layer on strain fields and transition energies in lens-shaped self-assembled SiGe/Si quantum dots. This study analyzes strain fields in and around quantum dots on the basis of the theory of linear elasticity. Strain fields are then incorporated into the steady-state effective-mass Schrödinger equation. Energy levels and wavefunctions of both electrons and holes are calculated. The calculated results of strain-induced phonon frequency are consistent with previous results obtained by Raman spectroscopy. Moreover, the calculated transition energy agrees well with previous experimental photoluminescence data. Numerical results also suggest that transition energy decreases as the template layer thickness increases. © *2008 American Institute of Physics*. [DOI: 10.1063/1.2891418]

I. INTRODUCTION

Due to three-dimensional quantum confinements, quantum dots (QDs) possess several interesting characteristics, including discrete energy levels and "atomlike" electronic states. These characteristics and their potential applications in optoelectronics have recently attracted substantial attention in the investigation of QDs.[1,2] Numerous studies have reported on InGaAs/GaAs and other group III-V quantum-dot heterostructures showing a wide range of dot sizes and shapes.[2–4] Group IV quantum-dot systems, such as SiGe/Si, are also interesting because of their potential applications in devices and their compatibility with silicon-based technology.[5–7]

Strain fields in and around self-assembled quantum dots (SAQDs) strongly affect optoelectronic properties of QDs. Hydrostatic strain shifts the edges of the conduction and the valence bands, while the uniaxial strain lifts the band degeneracy. Designing optoelectronic devices requires an accurate determination of the induced strain fields in both the quantum dot and the surrounding matrix. This information reveals how material parameters affect the conduction and valence bands and their curvatures, thereby altering the effective masses and transport properties.

Recently, Kurdi *et al.*[8] evaluated the strain fields of SiGe/Si SAQDs using valence force field theory. Makeev and co-workers[9,10] studied stress distribution in Ge/Si QDs using atomistic simulations. This paper investigates strain fields and energy levels in QDs using finite element method (FEM) to simulate the system of SiGe/Si QDs. The FEM is a very versatile and effective numerical method for accommodating different theories to model QDs at various levels of complexity. Previous studies[4] using the FEM showed good agreement with experimental photoluminescence data. This study analyzes strain fields induced by lattice mismatches in heterostructures on the basis of the theory of linear elasticity. The three-dimensional steady-state Schrödinger equation is then modified by incorporating the effects of strain fields into the carrier confinement potential and is analyzed by FEM numerically. The results include the energy levels and wavefunction spectra of SiGe/Si QDs. The calculated strain fields are also used to evaluate the strain-induced phonon frequencies which, along with the calculated transition energies, are compared against experimental data. Finally, this paper discusses the influence of template layer thickness on transition energies in SiGe/Si QDs.

II. PROBLEM STATEMENT

This paper considers a single lens-shaped SiGe QD buried in a Si matrix, as depicted schematically in Fig. 1. A thin template layer of $Si_{0.5}Ge_{0.5}$ is first grown on a (001) Si substrate. A thin Ge layer is then deposited on the template layer. Spontaneous coherent island formation then produces SAQDs. Finally, the quantum-dot islands are covered by a further deposition of the same material as the substrate. Numerical examples in this paper consider three different thicknesses of the $Si_{0.5}Ge_{0.5}$ template layer: $t=3$, 4, and 5 nm, all of which are less than the critical thickness.[11] The base diameter d and height h of the quantum dot are 70 and 21 nm, respectively. The thicknesses of the substrate and the capping

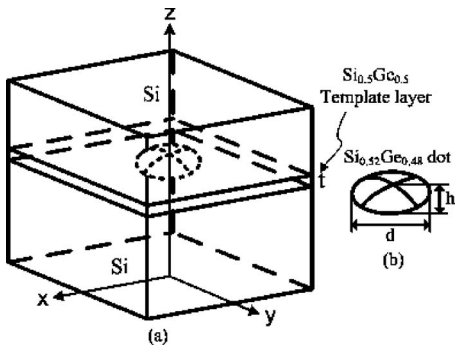

FIG. 1. (a) Schematics and geometries of Ge QD nanostructure. (b) d and h are the base diameter and height of the island, respectively.

[a]Electronic mail: mkkuo@ntu.edu.tw.

layer are 80 and 60 nm, respectively. The SiGe QD is assumed to have a uniform Ge concentration of 48%.[12]

III. STRAIN FIELD

Epitaxially grown semiconductor structures often consist of materials with different lattice constants. The mismatch of lattice constants creates strain fields in quantum-dot heterostructures, which affect the optoelectronic properties of quantum dots. In-plane lattice mismatch parameters[13] are defined as

$$(\varepsilon_0)_{xx} = (\varepsilon_0)_{yy} = \frac{a_s - a_d}{a_d} \tag{1}$$

where a_s and a_d are the lattice constants of the substrate (lower layer) and the quantum dots (upper layer) materials, respectively. The numerical values of lattice constant of the $Si_{1-c}Ge_c$ are set as $5.431+0.1992c+0.02733c^2$, where c is the Ge concentration.[14] In this example, the lattice constant of the substrate material (Si) is smaller than that of the template layer material ($Si_{0.5}Ge_{0.5}$). However, the lattice constant of the template-layer material exceeds that of the quantum-dot material ($Si_{0.52}Ge_{0.48}$). Therefore, the Si layer compresses the $Si_{0.5}Ge_{0.5}$ template layer, and the $Si_{0.5}Ge_{0.5}$ template layer puts tension on the $Si_{0.52}Ge_{0.48}$ dot. In other words, the $Si_{0.52}Ge_{0.48}$ dot will be less compressive than the $Si_{0.5}Ge_{0.5}$ template layer.

This paper assumes the deposition material adjusts its in-plane lattice constant to that of the substrate during epitaxial growth. It therefore induces an initial in-plane strain in the deposition material [i.e., $(\varepsilon_0)_{xx} = (\varepsilon_0)_{yy}$ in Eq. (1)]. The initial in-plane strain also accompanies an initial normal strain in the z axis (the direction of QD growth) in the deposition material due to Poisson's effect.[15,16] Based on the plane-stress assumption,[17] the initial out-of-plane strain $(\varepsilon_0)_{zz}$ leads to

$$(\varepsilon_0)_{zz} = -\frac{2C_{12}}{C_{11}}(\varepsilon_0)_{xx}. \tag{2}$$

Here, both Si and $Si_{1-c}Ge_c$ are considered as cubic materials. Each material has three independent elastic moduli: C_{11}, C_{12}, and C_{44}. The numerical values of elastic moduli used in this paper are taken from Ref. 18.

Notice that the lattice mismatch parameters defined in Eq. (1) are not yet the complete strain fields in the quantum-dot island. In fact, lattice mismatches will induce further elastic deformation in the entire nanostructure system, in the substrate, template layer, and the island, to ensure the equilibrium of the corresponding stresses. This paper regards the parameters $(\varepsilon_0)_{xx}$, $(\varepsilon_0)_{yy}$, and $(\varepsilon_0)_{zz}$ as the initial normal strains in the x-, y-, and z-directions, respectively. These initial strains in the template layer and the island induce further elastic strain fields in the entire SAQD system. Therefore, they serve as inputs in the following finite element analysis.

According to the theory of linear elasticity, the relationship between stresses σ_{ij}, total strains ε_{kl}, and initial strains can be expressed as

$$\sigma_{ij} = C_{ijkl}\left[\ \varepsilon_{kl} - \ (\varepsilon_0)_{kl}\right], \qquad i,j,k,l = x,y,z, \tag{3}$$

where C_{ijkl} is the component of the fourth-order tensor of elastic moduli and $(\varepsilon_0)_{kl}$ denotes the initial strain tensors described in Eqs. (1) and (2) with

$$(\varepsilon_0)_{kl} = 0 \qquad \text{for} \quad k \neq l. \tag{4}$$

This paper uses a finite element package (COMSOL Multiphysics) to analyze the linear elastic boundary value problem. This problem arises from the mismatch in lattice constants between the island, the template layer, and substrate materials. Analysis requires appropriate boundary conditions. The periodic symmetric argument requires that all nodes of the x- and y-outer surfaces are fixed against displacement in the normal direction. The bottom outer surface is fixed against displacement in the z-direction to avoid any possible rigid body translation. The upper surface is kept traction-free. The compatibilities of displacements across $Si_{0.5}Ge_{0.5}/Si$ and $Si_{0.52}Ge_{0.48}/Si_{0.5}Ge_{0.5}$ interfaces are satisfied automatically in finite element formulation with displacement fields used as basic unknowns.

Figures 2(a) and 2(b) show normal strain components ε_{xx} and ε_{zz}, respectively, of QD structure along the z-axis (the direction of QD growth) when the template layer is 5 nm thick. Kurdi *et al.* obtained similar tendency on strain distribution using the valence force field theory.[8] These strain components are not continuous across the $Si_{0.52}Ge_{0.48}/Si_{0.5}Ge_{0.5}$ and $Si_{0.5}Ge_{0.5}/Si$ interfaces, as one might expect from the theory of continuum mechanics. Notice from Fig. 2, inside the template layer and the dot, the strain fields ε_{xx} are compressive, while ε_{zz} are tensile. Moreover, inside the dot ε_{xx} is less compressive than that in the template layer. These results reveal that the lattice constants of the $Si_{0.5}Ge_{0.5}$ template layer and the $Si_{0.52}Ge_{0.48}$ quantum dot are larger than that of the Si substrate. The calculated strains have similar distributions but slightly differ in values for cases of different template layer thicknesses. In particular, the difference in ε_{xx} within the Si matrix (substrate and cap layer) increases as the thickness t increases, while the difference in ε_{zz} decreases.

The hydrostatic strain and uniaxial strain are defined respectively as

$$\varepsilon_h = \varepsilon_{xx} + \varepsilon_{yy} + \varepsilon_{zz} \quad \text{and} \quad \varepsilon_u = \varepsilon_{zz} - \frac{(\varepsilon_{xx} + \varepsilon_{yy})}{2}. \tag{5}$$

The calculated results show that the hydrostatic strain is negative in the template layer and the QD, while the uniaxial strain is positive. The strain in the Si layer is small since Si is much stiffer than SiGe. Figure 2(c) shows the hydrostatic stress, $\sigma_h = \sigma_{xx} + \sigma_{yy} + \sigma_{zz}$, along the z-axis (the direction of QD growth). The strain fields obtained here will serve as inputs for the confinement potentials and electric structure calculations in the following section. Makeev and coworkers report similar phenomena for a pyramidal Ge QD using atomistic simulation.[9,10]

It is also of interest to point out that several studies have used Raman scattering to characterize the strain and compo-

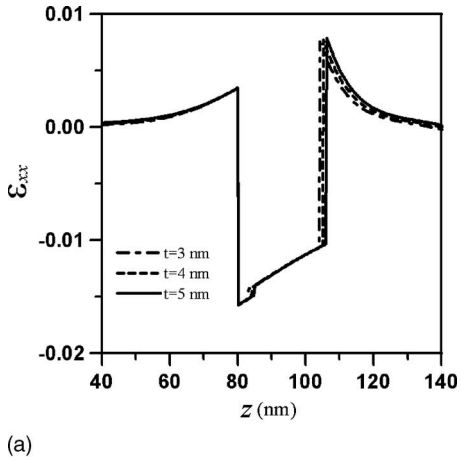

(a)

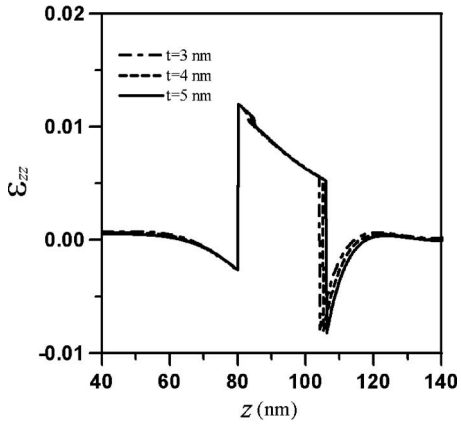

(b)

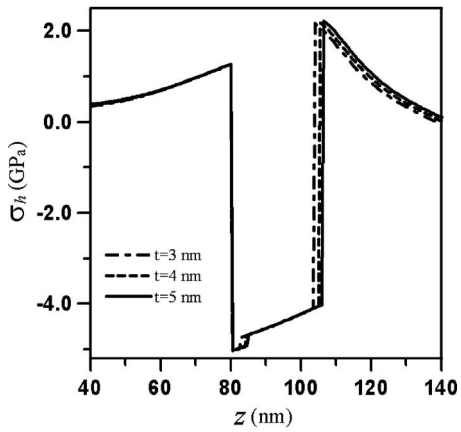

(c)

FIG. 2. (Color online)Strain components, (a) ε_{xx} and (b) ε_{zz}, and hydrostatic stress, (c) $\sigma_h=\sigma_{xx}+\sigma_{yy}+\sigma_{zz}$, plotted along the z-axis for various different template layer thicknesses.

sition of $Si_{1-c}Ge_c$ films.[12,19,20] The GeGe mode phonon frequency ω induced by QD strain components can be written as[19]

$$\omega = \omega_0 + \frac{1}{2\omega_0}(p\ \varepsilon_{zz} + 2\ q\ \varepsilon_{xx}), \tag{6}$$

where $\omega_0=0.5468\times10^{14}$ s^{-1} is the frequency of $Si_{0.52}Ge_{0.48}$ bulk alloys,[20] and the Ge deformation potentials p and q are -4.7×10^{27} and -6.167×10^{27} s^{-2}, respectively.[19] The averages of calculated strain fields,ε_{xx} and ε_{zz}, inside the quantum dot are -1.22×10^{-2} and 7.52×10^{-3}, respectively, for a template layer thickness of $t=5$ nm. Substituting these values directly into Eq. (6) leads to a phonon frequency ω of 296 cm^{-1}. For the sake of comparison the same procedure is used to calculate a hut-shaped QD with the same thickness of template layer, and the strain-induced phonon frequency is 297 cm^{-1} instead. It is well-known that the phonon frequency depends not only on built-in strain but also on the exact composition of the dots. Nevertheless, these calculated phonon frequencies here are very similar to an experimental GeGe mode phonon frequency.[12]

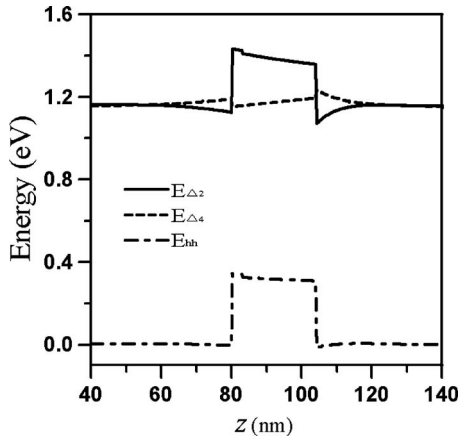

FIG. 3. Energy diagrams of the strained SiGe/Si QD heterostructures plotted along the z-axis for template layer thicknesses $t=5$ nm.

IV. TRANSITION ENERGY

The confinement potential V for strained quantum-dot heterostructures can be written as the sum of energy offsets of the unstrained conduction (or valence) band V_{band} and the strain-induced potential V_{strain},

$$V(\mathbf{r}) = V_{\text{band}}(\mathbf{r}) + V_{\text{strain}}(\mathbf{r}). \tag{7}$$

The difference in the bandgap energies of the constituent materials of the heterostructure determines the contribution of V_{strain}. Since strain effects induce an extra potential field V_{strain}, as suggested by the deformation potential theory,[21] any alteration in the band structure and optical properties of a quantum-dot system calls for further investigation. The electric material properties used in this study are taken from Ref. 18 and 22–26.

The confinement potentials in strained semiconductor QDs, including the strain-induced effects, are piecewise continuous functions of position. Figure 3 shows these potentials, along the z-axis (the direction of QD growth), for both electrons and holes. Notice that the Δ_4 valley in the Si matrix and the Δ_2 valley in the SiGe region are neglected. The conduction band offset at each interface has been calculated, and their values for the minima conduction band as deduced from $\Delta E_c^{\Delta_2-\Delta}(Si_{0.5}Ge_{0.5}/Si)$ and $\Delta E_c^{\Delta_4-\Delta}(Si_{0.5}Ge_{0.5}/Si)$ are around -36 and 28 meV, respectively, for different thicknesses t. On the other hand, $\Delta E_c^{\Delta_2-\Delta}(Si_{0.52}Ge_{0.48}/Si)=-91$, -93, and -95 meV, and $\Delta E_c^{\Delta_4-\Delta}(Si_{0.52}Ge_{0.48}/Si)=33$, 34, and 35 meV, for template layer thicknesses $t=3$, 4, and 5 nm, respectively. Thus, the band offset remains at a nearly constant value at

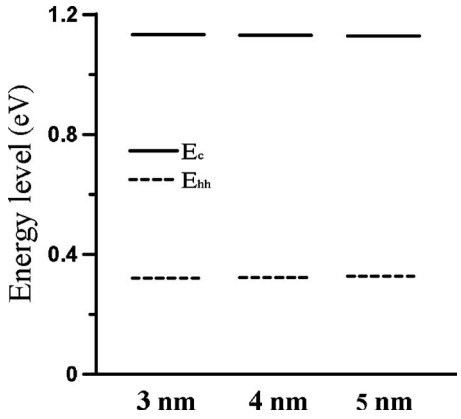

FIG. 4. Ground state energy levels of each band for different template layer thicknesses. The different lines correspond to the different energy bands.

the $Si_{0.5}Ge_{0.5}/Si$ interface. However, the band offset increases as the thickness t increases at the $Si_{0.52}Ge_{0.48}/Si$ interface.

The three-dimensional steady-state effective-mass Schrödinger equation helps to determine the behavior of individual carriers in quantum-dot nanostructures. This paper numerically analyzes the Schrödinger equation using the same finite element package used above. The ground state energy levels of the conduction as well as the heavy-hole and light-hole bands are calculated. Figure 4 shows these ground state energy levels for cases of different template layer thicknesses. Transition energy is defined as the difference between energy levels of the electron and the hole. These transition energies are related to the peaks of photoluminescence (PL) spectra. The optical conductivity peaks at particular wavelengths of light that are more strongly absorbed. The calculated fundamental transition energies are 0.804 and 0.810 eV for lens-shaped and hut-shaped QDs, respectively, with thickness $t=5$ nm, which agree well with the peak of experimental PL emission spectrum.[12] The transition energies of lens-shaped QDs for $t=3$ and 4 nm are 0.813 and 0.809 eV, respectively. These results suggest that the transition energy decreases as the template layer thickness increases.

Figure 5 shows the probability density function profiles $|\psi|^2$ for the ground state in a quantum-dot nanostructure. Figures 5(a) and 5(b) are the probability density function profiles of the electron state and the heavy-hole state, respectively, for the template layer thicknesses $t=5$ nm. In Fig. 5(a), the electrons are attracted to the top of the SiGe QD and are confined in the Si capping layer. This result might be due to the fact that a SiGe quantum-dot heterostructure is a typical type II transition material. In Fig. 5(b), the effect of the quantum-dot confines the hole in the template layer region right below the QD with a disklike shape. Other template layer thicknesses yield similar phenomena.

V. CONCLUSIONS

Based on the theory of linear elasticity, this paper analyzed the strain fields induced by lattice constant mismatches in SiGe/Si quantum-dot heterostructures using finite element methods. This study used the calculated strains to evaluate the strain-induced phonon frequencies and found that they were consistent with experimental phonon frequencies. Furthermore, the energy levels and wavefunction distribution have been obtained by analyzing the three-dimensional steady-state effective-mass Schrödinger equation. The calculated transition energies agreed well with previous experimental photoluminescence studies. Numerical results showed that transition energy decreases as the template layer thickness increases.

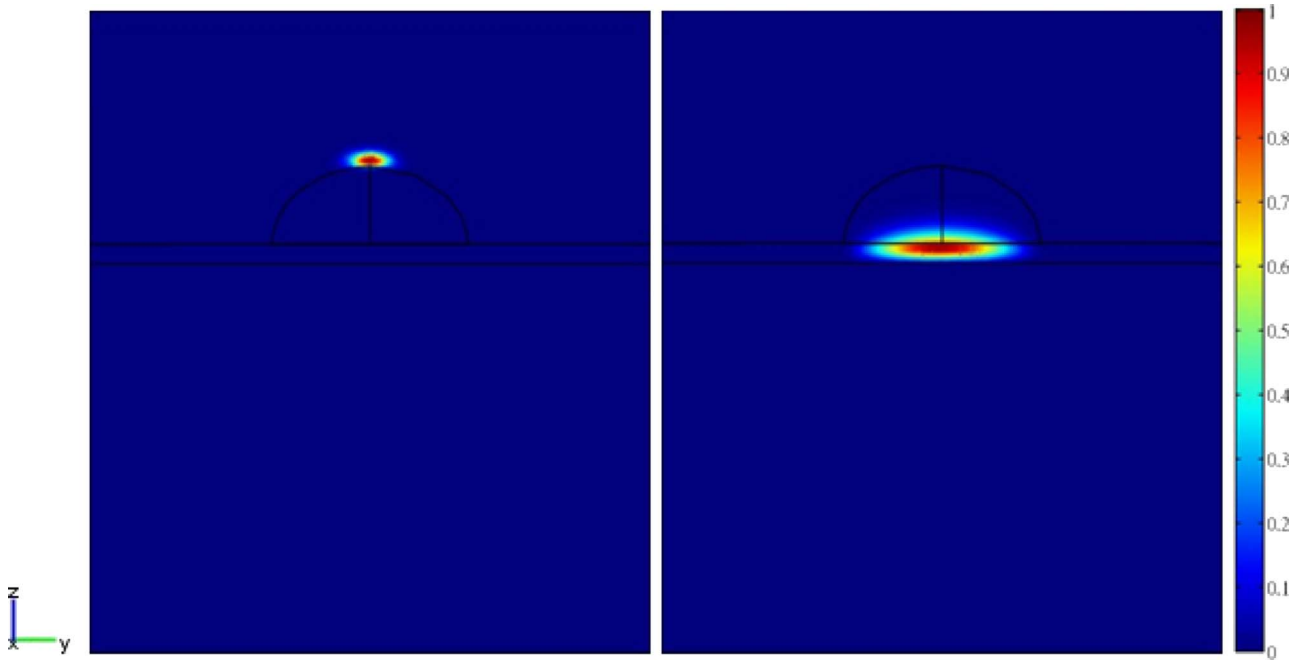

FIG. 5. (Color online) Probability density function profiles for energy levels of the ground state corresponding to (a) conduction band and (b) heavy-hole band for template layer thickness $t=5$ nm.

ACKNOWLEDGMENTS

This work is carried out in the course of research sponsored by the National Science Council of Taiwan under Grant Nos. NSC94-2212-E-002-004 and NSC95-2221-E-002-041-MY3.

[1]D. Bimberg, M. Grundmann, and N. N. Ledentsov, *Quantum Dot Heterostructures* (Wiley, West Sussex, 1999).
[2]P. Harrison, *Quantum Wells, Wires and Dots: Theoretical and Computational Physics* (Wiley, West Sussex, 2000).
[3]H. Pettersson, R. J. Warburton, J. P. Kotthaus, N. Carlsson, M. E. Seifcrt, and L. Samuelson, Phys. Rev. B **60**, R11289 (1999).
[4]M. K. Kuo, T. R. Lin, K. B. Hong, B. T. Liao, H. T. Lee, and C. H. Yu, Semicond. Sci. Technol. **21**, 626 (2006).
[5]V. Le. Thanh, P. Boucaud, D. Debarre, Y. Zheng, D. Bouchier, and J. M. Lourtioz, Phys. Rev. B **58**, 13115 (1998).
[6]P. H. Tan, K. Brunner, D. Bougeard, and G. Abstreiter, Phys. Rev. B **68**, 125302 (2003).
[7]B. V. Kamenev, L. Tsybeskov, J. M. Baribeau, and D. J. Lockwood, Appl. Phys. Lett. **84**, 1293 (2004).
[8]M. El. Kurdi, S. Sauvage, G. Fishman, and P. Boucaud, Phys. Rev. B **73**, 195327 (2006).
[9]M. A. Makeev and A. Madhukar, Phys. Rev. Lett. **86**, 5542 (2001).
[10]M. A. Makeev, W. Yu, and A. Madhukar, Phys. Rev. B **68**, 195301 (2003).
[11]F. Schäeffler, Semicond. Sci. Technol. **12**, 1515 (1997).
[12]I. Berbezier, M. Descoins, B. Ismail, H. Maaref, and A. Ronda, J. Appl. Phys. **98**, 063517 (2005).
[13]L. B. Freund, Int. J. Solids Struct. **37**, 185 (2000).
[14]V. T. Bublik, S. S. Gorelik, A. A. Zaitsev, and A. Y. Polyakov, Phys. Status Solidi B **65**, K79 (1974).
[15]M. K. Kuo, T. R. Lin, B. T. Liao, and C. H. Yu, Physica E **26**, 199 (2005).
[16]T. R. Lin, M. K. Kuo, B. T. Liao, and K. P. Hung, Bull. Coll. Eng., Natl. Taiwan Univ. **91**, 3 (2004).
[17]John H. Davies, D. M. Bruls, J. W. A. M. Vugs, and P. M. Koenraad, J. Appl. Phys. **91**, 4171 (2002).
[18]M. E. Levinshtein, S. L. Rumyantsev, and M. S. Shur, *Properties of Advanced Semiconductor Materials* (Wiley, New York, 2001).
[19]J. Groenen, R. Carles, S. Christiansen, M. Albrecht, W. Dorsch, H. P. Strunk, H. Wawra, and G. Wagner, Appl. Phys. Lett. **71**, 3856 (1997).
[20]H. K. Shin, D. J. Lockwood, and J. M. Baribeau, Solid State Commun. **114**, 505 (2000).
[21]S. L. Chuang, *Physics of Optoelectronic Devices* (Wiley, New York, 1995).
[22]G. C. Van de Walle and R. M. Martin, Phys. Rev. B **34**, 5621 (1986).
[23]G. C. Van de Walle, Phys. Rev. B **39**, 1871 (1989).
[24]D. J. Paul, Semicond. Sci. Technol. **19**, R75 (2004).
[25]M. M. Rieger and P. Vogl, Phys. Rev. B **48**, 14276 (1993).
[26]L. Yang, J. R. Watling, R. C. W. Wilkins, M. Borici, J. R. Barker, A. Asenov, and S. Roy, Semicond. Sci. Technol. **19**, 1174 (2004).